

Facial Expression Classification Using Rotation Slepian-based Moment Invariants

Cuiming Zou* and Kit Ian Kou†

Department of Mathematics, Faculty of Science and Technology, University of Macau,
Macao, China

Abstract

Rotation moment invariants have been of great interest in image processing and pattern recognition. This paper presents a novel kind of rotation moment invariants based on the Slepian functions, which were originally introduced in the method of separation of variables for Helmholtz equations. They were first proposed for time series by Slepian and his coworkers in the 1960s. Recent studies have shown that these functions have a good performance in local approximation compared to other approximation basis. Motivated by the good approximation performance, we construct the Slepian-based moments and derive the rotation invariant. We not only theoretically prove the invariance, but also discuss the experiments on real data. The proposed rotation invariants are robust to noise and yield decent performance in facial expression classification.

Keywords: Orthogonal moment; Slepian functions; rotation invariants

1 Introduction

Moment invariants have aroused great interest in image processing and pattern recognition in the last 50 years [3]. The first kind of moment invariants was presented by Hu [4] in pattern recognition. Since then, the applications have been reported in a variety of problems, such as image watermark [5], gesture recognition [6], noise analysis [7] and color image [8]. Invariance with respect to translation, rotation and scaling is required in almost all practical applications, because the article should be correctly acquainted, regardless of its position and orientation in the site and of the object-to-camera distance. Furthermore, the translation, rotation and

*zoucuiming2006@163.com

†Corresponding author: kikou@umac.mo

scaling model is a ample approximation of the actual image deformation if the location is flat and almost vertical to the optical axis. Therefore, much attention has been paid to translation, rotation and scaling invariants. While translation and scaling invariants can be derived in a instinctive way, derivation of invariants to rotation is far more complicated.

The moment M_{mn} of a weighting kernel ϕ_{mn} and the intensity function f is given by [1]

$$M_{mn} := \iint_{\mathbb{R}^2} \phi_{mn}(x, y) f^*(x, y) dx dy, \quad (1.1)$$

where M_{mn} ($m, n = 0, 1, 2, 3, \dots$) are the projections of f onto the space spanned by $\{\phi_{mn}\}_{m,n=0}^{\infty}$. Moments M_{mn} can be grossly divided into non-orthogonal moments and orthogonal moments [9]. The classical non-orthogonal moments include geometric moments, rotational moments and complex moments. The geometric moments are projections of the image onto the space spanned by monomials, i.e., $\phi_{mn}(x, y) = x^m y^n$ [2]. The complex moments have the similar structure as geometric moments except for $\phi_{mn}(x, y) = (x + \mathbf{i}y)^m (x + \mathbf{i}y)^n$ [10]. The rotational moments are defined directly in polar coordinates, i.e., $\phi_{mn}(r, \theta) = r^m e^{\mathbf{i}n\theta}$ [11].

From the theory of algebraic invariants, the non-orthogonal basis will lead to the information redundancy [1]. In order to overcome the shortcomings of this problem, Teague [12] introduced the orthogonal moments by orthogonal polynomials in 1980. Some popular orthogonal moments are Legendre and Zernike moments [13]. Legendre moments [14] in Cartesian coordinate are generated by $\phi_{mn}(x, y) := P_m(x)P_n(y)$, where $P_m(x)$ is the m th order of Legendre polynomial. The finite energy signal $f(x, y)$ can be reconstructed by its Legendre moments [12]. While Zernike moments [15] were generated by $\phi_{mn}(r, \theta) := R_m(r)e^{-\mathbf{i}n\theta}$, where $R_m(r)$ is the m th order Zernike radial polynomial. Other kinds of continuous orthogonal moments have the similar structure and properties as the above moments, such as pseude-Zernike moments [16], Chebyshev-Fourier moments [17], Exponent-Fourier moments [18]. There are some discrete orthogonal moments in the literature, such as Tchebichef, dual Hahn, Racah moments and so on, which can be effectively solved a lots of physical problems [19].

The paper proposes a novel kind of moments on a disk. They are constructed as products of a radial factor (Slepian functions) and angular factor (harmonic function). We named it as Slepian-based moments (SMs) and used SMs to construct rotation invariants. Slepian functions are a set of functions derived by timelimiting and lowpassing, and a second timelimited operation, as originally proposed for time series by Slepian and coworkers, in the 1960s [21]. They possess many remarkable properties, such as orthogonal basis of both square integrable space of finite interval and the Paley-Wiener space of bandlimited functions on the real line [20, 21, 22]. They are the most energy concentrated functions, among the set of bandlimited functions with a given bandwidth, on fixed space domain [22]. Since the energy concentrated property on fixed space domain, the Slepian basis has good performance in local approximation compared to other approximation basis, such as Fourier basis and polynomials [20]. This raises the question of whether they yield decent performance in image processing.

The aim of the article is to answer this question by applying the Slepian functions as the kernel ϕ_{mn} of moment M_{mn} . To the best of the authors' knowledge, the study of moment invariants under the Slepian functions has not been carried out. In the present study we construct

the SMs and derive the rotational invariants. We show that the numerical computation of SMs is $O(MN \log_2 N)$ and apply these new invariants in facial expression classification. Our experiments demonstrate that the rotational invariants are robust to image noise and have good recognition capabilities in facial expression classification.

The paper is organized as follows. Section 2 is devoted to necessary preliminaries. In Section 3 the rotation invariants are derived by the proposed Slepian-based moments. In Section 4, the extended Conh-Kanade database (CK+) [25] is used to test the rotation invariance and the robustness of the proposed variants to noise. The proposed SMs invariants are also applied as features to facial expression classification. Finally, we draw a conclusion in Section 5.

2 Preliminary

In the following, the *image* f denotes a piecewise continuous complex-valued function defined on a compact domain of 2D space ($D \subset \mathbb{R}^2$) [1]. The image function $g(x, y)$ in Cartesian coordinate can be changed to polar coordinate as $g(r \cos \theta, r \sin \theta)$. To simplify the notation, denote $f(r, \theta)$ the polar coordinate of an image in the following.

2.1 Moment in polar coordinates

Definition 2.1 *Moment M_{mn} of an image f in polar coordinates is defined by*

$$M_{mn} := \iint_D R_{mn}(r) e^{-in\theta} f^*(r, \theta) r dr d\theta, \quad (2.1)$$

where m, n are non-negative integers, $r = m + n$ is the order of M_{mn} and $(\cdot)^*$ means the complex conjugate operation. (r, θ) are the polar coordinates. $R_{mn}(r)$ is a radial part and $e^{-iq\theta}$ is the angular factor. The area of $D := \{(r, \theta) : 0 \leq r \leq 1, 0 \leq \theta \leq 2\pi\}$.

There are many moments defined on a disk, for example,

- the Zernike moments of the $m + n$ -th order are defined as the radial part $R_m(r)$ is the Zernike polynomials;
- the Fourier-Mellin moments have the similarly definition as $R_m(r) = r^{n-2}$;
- the orthogonal Fourier-Mellin moments defined as $R_m(r)$ is a linear combination of the factor r^i , $i = 0, 1, 2, \dots$, i.e.,

$$R_m(r) = \sum_{s=0}^m (-1)^{m+s} \frac{(m+s+1)!}{(m-s)!s!(s+1)!} r^s. \quad (2.2)$$

This radial functions $R_m(r)$ are modified by r^i , $i = 0, 1, 2, \dots$

Numerous types of moments with orthogonal polynomials have been described in different area of practical applications [1]. The finite energy image f can be reconstructed by these orthogonal polynomials

$$f(r, \theta) = \sum_{m,n=0}^{\infty} M_{mn} R_{mn}(r) e^{-in\theta}. \quad (2.3)$$

It minimizes the mean-square error when using only a finite set of moments on the reconstruction [1].

2.2 Slepian-based moment

Similar to the definition of moment in polar coordinates, such as Zernike moments, Fourier-Mellin moments, orthogonal Fourier-Mellin moments. We will change the radial part to a special function i.e., Slepian functions. The moments we defined by this functions is called Slepian-based moments. Now we first introduce the Slepian functions in continuous form and discrete form.

2.3 Slepian functions in continuous form

The Slepian functions, originated from the context of separation of variables for the Helmholtz equation in spheroidal coordinates, have been extensively used for a variety of physical and engineering applications [1, 22]. It is remarkable that the Slepian functions $\{\psi_m\}_{m,n=0}^{\infty}$ [22] are also the eigenfunctions of the integral equations

$$\lambda_m \psi_m(x) = \int_{-1}^1 \psi_m(u) e^{icxu} du, \quad (2.4)$$

where the integral domain is symmetric and c is a given positive number and λ_m is the real-valued eigenvalue corresponding to ψ_m in Eq. (2.4).

This kind of functions have many good properties, the most important properties are list as follows: given a real $c > 0$, there are a countably infinite set of $\{\psi_n(x)\}_{n=0}^{\infty}$ and their corresponding eigenvalues $\{\lambda_n\}_{n=0}^{\infty}$

- The eigenvalues λ_n 's are real and monotonically decreasing in $(0, 1)$:

$$\lambda_0 \geq \lambda_1 \geq \lambda_2 \geq \dots, \quad (2.5)$$

and such that $\lim_{n \rightarrow \infty} \lambda_n = 0$;

- The $\{\psi_n(x)\}_{n=0}^{\infty}$ are orthogonal in $[-1, 1]$:

$$\int_{-1}^1 \psi_n(x) \overline{\psi_m(x)} dx = \lambda_n \delta_{mn}; \quad (2.6)$$

- The $\{\psi_n\}_{n=0}^\infty$ are orthonormal in \mathbb{R}^2 :

$$\int_{\mathbb{R}^2} \psi_n(x) \overline{\psi_m(x)} dx = \delta_{mn}. \quad (2.7)$$

The Slepian functions are also an orthogonal basis of both integrable in the finite interval and the Paley-Wiener space of bandlimited functions on the real line [21, 22, 20]. The Slepian functions have been proved as the most energy concentrated functions, among the set of bandlimited functions with a given bandwidth, on fixed space domain [22]. Since the energy concentrated property on fixed space domain, the Slepian basis has good performance in local approximation compared to other approximation basis, such as Fourier basis and polynomials [20]. This raises the question of whether they yield decent performance in image processing.

2.4 Slepian functions in discrete form

Recently, there has been a growing interest in developing numerical methods using Slepian functions as basis functions. The discrete Slepian functions are developed by Slepian at first [23], which is also called the discrete prolate spheroidal sequences (DPSS). For given N the number of length of the sequences and W the bandwidth of the sequences, the DPSS $v_n^{(k)}(N, W)$ is defined as the solution to the system of equations

$$\sum_{m=0}^{N-1} \frac{\sin 2\pi(n-m)}{\pi(n-m)} v_m^{(k)}(N, W) = \lambda_k(N, W) v_n^{(k)}(N, W), \quad (2.8)$$

where $k = 0, 1, 2, \dots, N-1$, $\lambda_k(N, W)$ is the eigenvalue for the DPSS $v_n^{(k)}(N, W)$. The DPSS are also have the double orthogonal properties

$$\sum_{m=0}^{N-1} v_m^{(s)}(N, W) v_m^{(t)}(N, W) = \lambda_s(N, W) \sum_{m=0}^{N-1} v_m^{(s)}(N, W) v_m^{(t)}(N, W) = \delta_{st}, \quad (2.9)$$

where $\delta_{st} = 0$ for $s \neq t$ and $\delta_{st} = 1$ if $s = t$. Here, $s, t = 0, 1, 2, \dots, N-1$.

Denote

$$f_k(N, W, u) := \epsilon_k \sum_{m=0}^{N-1} v_m^{(k)}(N, W) e^{-i\pi(N-1-2m)u}, \quad (2.10)$$

where $\epsilon_k = 1$ for k even and $\epsilon_k = 0$ for k odd. and the coefficient $v_m^{(k)}(N, W)$ has

$$v_m^{(k)}(N, W) = \frac{1}{\epsilon_k} \int_{-\frac{1}{2}}^{\frac{1}{2}} f_k(N, W, u) e^{i\pi(N-1-2m)u} du. \quad (2.11)$$

We may also obtain that

$$v_m^{(k)}(N, W) = \frac{1}{\epsilon_k \lambda_k(N, W)} \int_{-W}^W f_k(N, W, u) e^{i\pi(N-1-2m)u} du. \quad (2.12)$$

Let $W = 1$, the above formulary is already the Slepian functions in the integer points, i.e., $x = N-1-2m$ in Eq. (2.4).

2.5 Slepian-based moments

Since we have known the Slepian functions in continuous and discrete forms, we can apply them in moment theory. To the best of the authors knowledge, the study of moment invariants under the Slepian functions has not been carried out. We are now ready to construct a new kind of moment related to this Slepian functions, which is named as Slepian-based moment. The definition is similar to the definition of the moment in polar coordinates, while the radial function changes to the Slepian functions.

Definition 2.2 *The Slepian-based moments (SMs) of an image $f(r, \theta)$ is defined by*

$$S_{mn} := \iint_D \psi_m(r) e^{-in\theta} f^*(r, \theta) r dr d\theta, \quad (2.13)$$

where m, n are non-negative integers and $r = m + n$ is the order of S_{mn} . The radial functions $\{\psi_m\}_{m=0}^\infty$ are the Slepian functions satisfying Eq. (2.4).

The bandlimited functions $f(r, \theta)$ can be represented by the Slepian series [22]

$$f(r, \theta) = \sum_{m=0}^{\infty} \sum_{n=0}^{\infty} S_{mn} \psi_m(r) e^{-in\theta}. \quad (2.14)$$

Moreover, it can also be approximated well by linear combinations of the Slepian functions of order $M + N$ [22].

$$\tilde{f}(r, \theta) = \sum_{m=0}^M \sum_{n=0}^N S_{mn} \psi_m(r) e^{-in\theta}. \quad (2.15)$$

3 Rotation invariants

In this section, the use of SMs in in polar coordinates on $D = \{(r, \theta) : 0 \leq r \leq 1, 0 \leq \theta \leq 2\pi\}$ in the capacity of rotation invariants is discussed. For any image function $f(r, \theta)$ in polar coordinate.

3.1 Rotation invariance

Let $f'(r, \theta)$ be a rotated version of $f(r, \theta)$ with a rotation angle α , i.e., $f'(r, \theta) = f(r, \theta + \alpha)$. The S'_{mn} of $f'(r, \theta)$ and S_{mn} of $f(r, \theta)$ have relations

$$\begin{aligned} S'_{mn} &= \int_0^1 \int_0^{2\pi} \psi_m(r) e^{-in\theta} f^*(r, \theta + \alpha) \sqrt{r} dr d\theta \\ &= e^{im\alpha} \int_0^1 \int_0^{2\pi} \psi_m(r) e^{-in\theta} f^*(r, \theta) \sqrt{r} dr d\theta \\ &= e^{im\alpha} S_{mn}. \end{aligned}$$



Figure 1: Examples in the CK+ database. Facial images of 6 emotions: Fear, Surprise, Sadness, Disgust, Anger, and Happy.

The above equation implies rotation invariance of the S_{mn} while the phase is shifted by α . Taking absolute value on both sides of $S'_{mn} = e^{im\alpha} S_{mn}$, we have

$$|S'_{mn}| = |e^{im\alpha} S_{mn}| = |S_{mn}| =: \Phi_{mn}. \quad (3.1)$$

Thus, Φ_{mn} is a rotation invariant induced by S_{mn} . The rotation invariance is the most important invariance for the moment theory. Since we find these rotation invariants, we can use them to the practical applications. In the following, we will show the numerical computation for this kind of moments.

3.2 Numerical computation

Considering a discrete $M \times N$ image $g(M, N)$, we first change the Cartesian coordinates to polar coordinates [?]. For a polar coordinates image $f(r, \theta)$, calculate the discrete form of Eq. (2.13) in polar coordinates as follows

$$\begin{aligned} S_{mn} &:= \sum_{r=0}^1 \sum_{\theta=0}^{2\pi} \psi_m(r) e^{-in\theta} f^*(r, \theta) r \Delta\theta \Delta r \\ &= \sum_{r=0}^1 \psi_m(r) r \left(\sum_{\theta=0}^{2\pi} e^{-im\theta} f^*(r, \theta) \Delta\theta \right) \Delta r, \end{aligned} \quad (3.2)$$

where the expression inside the parenthesis can be considered as a discrete form of one-dimensional Fourier transform in θ . Therefore, we can use the FFT in matlab to obtain fast computation. As for numerical computation of the function $\psi_m(r)$, please refer to the programs of DPSS in [23]. The total computing complexity of S_{mn} is $O(MN \log_2 N)$.

4 Experimental results

This section is devoted to verify the performance of SMs and SMs rotation invariants in facial expression classification, which is a kind of problem in facial classification [24]. Specifically, the extended Conh Kanade database (CK+) [25] is used for the experiments.

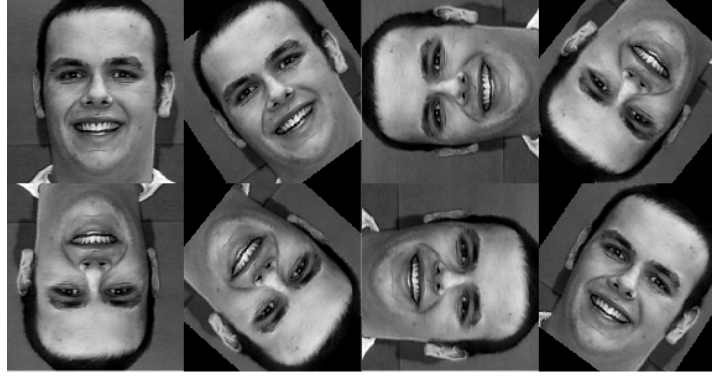


Figure 2: Examples of an image in 8 orientations: 0° , 35° , 90° , 140° , 180° , 230° , 270° , and 325° .

Table 1: Φ_{mn} and standard deviations for the same image in 8 orientations in Figure 2.

α	$\Phi_{1,1}$	$\Phi_{1,2}$	$\Phi_{2,1}$	$\Phi_{2,2}$	$\Phi_{2,3}$	$\Phi_{3,2}$	$\Phi_{3,4}$	$\Phi_{4,1}$	$\Phi_{4,3}$	$\Phi_{4,5}$
0°	0.0517	0.0764	0.0733	0.0955	0.0476	0.1202	0.1559	0.2366	0.3316	0.0881
35°	0.0612	0.0750	0.0770	0.0933	0.0461	0.1185	0.1514	0.2510	0.3474	0.0984
90°	0.0724	0.0742	0.0855	0.0926	0.0479	0.1175	0.1553	0.2280	0.3295	0.0864
140°	0.0612	0.0754	0.0764	0.0929	0.0455	0.1172	0.1429	0.2411	0.3277	0.0959
180°	0.0724	0.0740	0.0815	0.0914	0.0446	0.1172	0.1471	0.2672	0.3645	0.1085
230°	0.0612	0.0748	0.0766	0.0926	0.0458	0.1175	0.1426	0.2407	0.3273	0.0957
270°	0.0519	0.0764	0.0688	0.0942	0.0444	0.1196	0.1478	0.2735	0.3659	0.1117
325°	0.0611	0.0753	0.0768	0.0934	0.0462	0.1186	0.1514	0.2509	0.3489	0.0978
<i>std.</i>	0.0073	0.0008	0.0047	0.0011	0.0012	0.0011	0.0047	0.0144	0.0151	0.0082

4.1 Image data

The CK+ is a kind of database to detect individual facial expressions [25]. We consider the posed emotion-specified expressions, which have 593 image sequences from 123 subjects. These sequences have a nominal emotion label based on the subject's impression of each of the basic emotion categories: Fear, Surprise, Sadness, Disgust, Anger, and Happy. Examples of the CK+ are given in Figure 1.

4.2 Rotation invariance and noise

In Section 3, we have proved that Φ_{mn} are rotation invariants based on S_{mn} for different m, n . In this part, we will compute the Φ_{mn} for the same image with different orientations to validate the rotation invariance of Φ_{mn} numerically. The rotation transform with the angle θ for an image is



Figure 3: Examples of an image in 8 orientations with 30db Gaussian noise.: 0° , 35° , 90° , 140° , 180° , 230° , 270° , and 325° .

as follows

$$\begin{pmatrix} x' \\ y' \end{pmatrix} = \begin{pmatrix} \cos \theta & -\sin \theta \\ \sin \theta & \cos \theta \end{pmatrix} \begin{pmatrix} x \\ y \end{pmatrix}.$$

Figure 2 shows an image with 8 different orientations. Since the different rotation will change the size of images, we just show the rotational images with the same size as the original one. In Table 1 we show 10 values of Φ_{mn} with $m = 1, 2, 3, 4$ and $n = 1, 2, 3, 4, 5$ for every rotated image. The last row of Table 1 is the standard deviation (*std.*) of Φ_{mn} in different orientations. Since all of the *std.* for different Φ_{mn} are very small, it shows that the value of Φ_{mn} is stable. This result is consistent with the proposed theory of the rotational invariance of Φ_{mn} .

Now we evaluate the robustness of the Φ_{mn} to noise [26]. As an example in Figure 3 we show the mostly widely used Gaussian noise to the same images in Figure 2. In Table 2 we experiment the values of Φ_{mn} for the images in Figure 2 with 30db Gaussian noise for $m = 1, 2, 3, 4$ and $n = 1, 2, 3, 4, 5$. Even all of the *std.* in Table 2 for different Φ_{mn} is slight larger than the *std.* in Table 1, but they are also very small. It shows that for the same image with Gaussian noise, the value of Φ_{mn} s are stable. We can now find that the value of Φ_{mn} of same image with noise are basically the same as the value of Φ_{mn} in Table 1. That is, the noise has little influence to the Φ_{mn} .

4.3 Facial expression classification

At last, we aim to apply the Φ_{mn} with different m, n as feature vectors to the problem of emotion-specified expression classification. We use Φ_{mn} as features to classify the different facial expression for the same subject.

The support vector machine (SVM) is applied to classify the same subject with six different emotion-specified expressions. The SVM was proposed by Vapnik [27] as a very effective method for multi-class classification. Here, we only use the first 10 Slepian functions to construct a feature vector with 100 elements of the images. We choose 5 sequences in CK+

Table 2: Φ_{mn} and standard deviations for the images in Figure 2 with 30db Gaussian noise.

α	$\Phi_{1,1}$	$\Phi_{1,2}$	$\Phi_{2,1}$	$\Phi_{2,2}$	$\Phi_{2,3}$	$\Phi_{3,2}$	$\Phi_{3,4}$	$\Phi_{4,1}$	$\Phi_{4,3}$	$\Phi_{4,5}$
0°	0.0536	0.0782	0.0720	0.0973	0.0456	0.1202	0.1568	0.2414	0.3266	0.0884
35°	0.0632	0.0718	0.0779	0.0921	0.0467	0.1207	0.1530	0.2431	0.3516	0.1039
90°	0.0769	0.0753	0.0869	0.0926	0.0488	0.1171	0.1556	0.2305	0.3393	0.0856
140°	0.0667	0.0748	0.0761	0.0956	0.0482	0.1203	0.1445	0.2360	0.3263	0.0970
180°	0.0733	0.0729	0.0788	0.0903	0.0438	0.1150	0.1495	0.2766	0.3674	0.1053
230°	0.0605	0.0758	0.0762	0.0909	0.0462	0.1172	0.1433	0.2348	0.3250	0.0908
270°	0.0506	0.0760	0.0695	0.0942	0.0459	0.1201	0.1448	0.2706	0.3693	0.1137
325°	0.0594	0.0705	0.0750	0.0939	0.0467	0.1200	0.1493	0.2473	0.3402	0.0996
<i>std.</i>	0.0085	0.0024	0.0048	0.0022	0.0015	0.0020	0.0048	0.0159	0.0168	0.0089

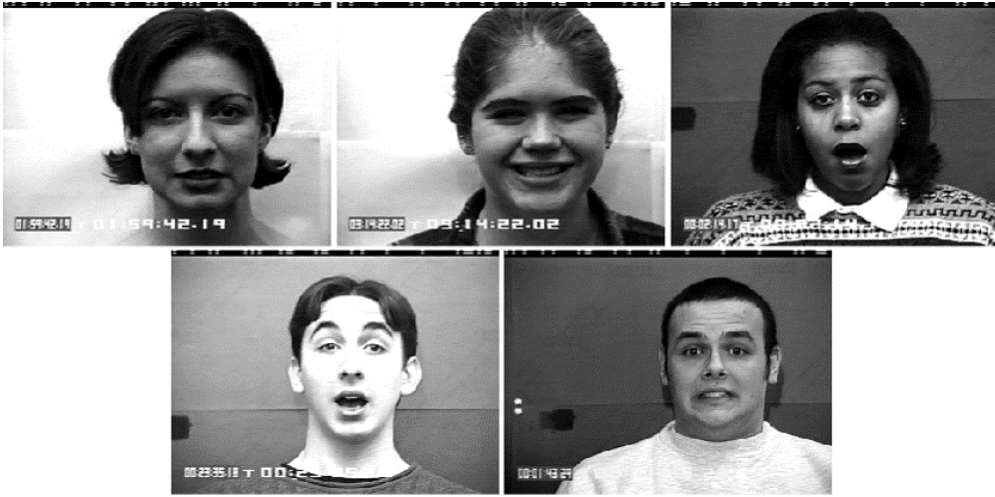


Figure 4: Examples of the 5 subjects in CK+ database used for classification, from left to right: S010, S011, S022, S037, and S050.

database in Figure 4, which are in the files of S010, S011, S022, S037, and S050. Each sequences has been marked by 6 kinds of emotion-specified expressions as Figure 1, i.e., fear: 1, surprise: 2, sadness: 3, disgust: 4, anger: 5, and happy: 6. For each expression we random choose 8 images in our experiments, which means we have $6 * 8$ images for each subject. Then we use a part of them for training and the rest images for testing and get the percentage of classification each time. Since we randomly choose a part of them to get the percentage of accuracy, we repeat 10 times for each subject and we take the average number for classification in Table 3. For 50% training means, for the same subject with 48 images, 24 images are using to train in the SVM. From Table 3, we find that only 30% images are needed to train SVM and the percentage can be reached very high. At the same time, we must take care to the fact that only 10 Slepian functions used to construct the feature vectors for each subject. Thanks to the theory of Slepian functions [21, 22, 23], only the lower order Slepian-based moments are needed in our

Table 3: Classification accuracy for 5 subjects with 6 different facial expressions using different percent of training images.

$p\%$		S010	S011	S022	S037	S050
20	<i>mean</i>	0.6590	0.3872	0.4103	0.4795	0.4615
	<i>std.</i>	0.2271	0.1370	0.2033	0.1817	0.1781
30	<i>mean</i>	0.9588	0.7588	0.8118	0.9735	0.9382
	<i>std.</i>	0.0397	0.1453	0.0638	0.0352	0.0596
40	<i>mean</i>	0.9897	0.7966	0.8793	0.9690	0.9793
	<i>std.</i>	0.0233	0.0550	0.0592	0.0343	0.0291
50	<i>mean</i>	0.9833	0.8875	0.8833	0.9833	0.9958
	<i>std.</i>	0.0291	0.0483	0.0430	0.0215	0.0132

experiments and they already contain the mostly information for the emotion-specified image.

5 Conclusion

This paper develops a novel kind of moments based on the Slepian functions. Motivated by the excellent properties of the Slepian functions, we define the Slepian-based moments and the corresponding moment rotation invariants. We notice that the study of moments combining with Slepian functions has not been carried out in the literature. These rotational invariants are tested as features to classify the emotion-specified expressions in the CK+ database and the experimental results give a positive result in terms of the accuracy of classification. The current study only shows the moment invariants with respect to rotation suitable for emotion-specified recognition. The construction of the generalized invariant basis to affine and projective transforms will be considered in the upcoming paper.

References

- [1] J. Flusser, T. Suk, and B. Zitová, *Moments and moment invariants in pattern recognition*. Wiley, 2009.
- [2] R. Mukundan and K. Ramakrishnan, *Moment Functions in Image Analysis-Theory and Application*. World Scientific; Singapore, 1998.
- [3] C. Teh and R. Chin, “On image analysis by the method of moments,” *IEEE Transactions on Pattern Analysis and Machine Intelligence*, vol. 10, no. 4, pp. 496–513, Apr. 1988.
- [4] M. Hu, “Visual pattern recognition by moment invariants,” *IRE Transactions on Information Theory*, vol. 8, no. 2, pp. 70–74, Feb. 1962.

- [5] H. Kim and H. Lee, "Invariant image watermark using Zernike moments," *IEEE Transactions on Circuits and Systems for Video Technology*, vol. 13, no. 8, pp. 766–775, Aug. 2003.
- [6] S. Priyal and P. Bora, C. Teh and R. Chin, "A study on static hand gesture recognition using moments," *2010 International Conference on Signal Processing and Communications (SPCOM)*, pp. 1–5, Jul. 2010.
- [7] A. Hyvarinen, "Gaussian moments for noisy independent component analysis," *IEEE Signal Processing Letters*, vol. 6, no. 6, pp. 145–147, Jun. 1999.
- [8] S. Pei and C. Cheng, "Color image processing by using binary quaternion-moment-preserving thresholding technique," *IEEE Transactions on Image Processing*, vol. 8, no. 5, pp. 614–628, May 1999.
- [9] H. Shu, L. Luo, and J. Coatrieux, "Moment-based approaches in imaging," *IEEE Engineering in Medicine and Biology Magazine*, vol. 26, no. 5, pp. 70–74, Sep. 2007.
- [10] H. Ren, Z. Ping, W. Bo, W. Wu, and Y. Sheng, "Multi-distortion invariant image recognition with radial harmonic fourier moments," *Optical Society of America A.*, vol. 20, pp. 631–637, 2003.
- [11] A. Mostafa, S. Yaser, and D. Psaltis, "Image Normalization by Complex Moments," *IEEE Transactions on Pattern Analysis and Machine Intelligence*, vol. PAMI-7, no. 1, pp. 46–55, Jan. 1985.
- [12] M. Teague, "Image analysis via the general theory of moments," *Optical Society of America*, vol. 70, pp. 920–930, 1980.
- [13] H. Zhu, "Image representation using separable two-dimensional continuous and discrete orthogonal moments," *Pattern Recognition Letters*, vol. 45, pp. 1540–1558, 2012.
- [14] M. Khalid, "Exact legendre moment computation for gray level images," *Pattern Recognition*, vol. 40, pp. 3597–3605, 2007.
- [15] L. Wang and G. Healey, "Using zernike moments for the illumination and geometry invariant classification of multispectral texture," *IEEE Transactions on Image Processing*, vol. 7, no. 2, pp. 196–203, Feb. 1998.
- [16] T. Xia, H. Zhu, H. Shu, P. Haignon, and L. Luo, "Image description with generalized pseudo-zernike moments," *Optical Society of America A.*, vol. 24, no. 1, pp. 50–59, 2007.
- [17] Z. Ping, R. Wu, and Y. Sheng, "Image description with chebyshev-fourier moments," *Optical Society of America A.*, vol. 19, pp. 1748–1754, 2002.
- [18] H. Hu, Y. Zhang, C. Shao, and Q. Ju, "Orthogonal moments based on exponent functions: Exponent-fourier moments," *Pattern Recognition*, vol. 47, pp. 2596–2606, 2014.

- [19] R. Mukundan, “Some computational aspects of discrete orthonormal moments,” *IEEE Transactions on Image Processing*, vol. 13, no. 8, pp. 1055–1059, Aug. 2004.
- [20] A. Jeffrey and D. L. Joseph, *Duration and bandwidth limiting: Prolate Functions, Sampling, and Applications*. Springer Science and Business Media, 2011.
- [21] D. Slepian and H. Pollak, “Prolate spheroidal wave functions, fourier analysis, and uncertainty–I,” *Bell System Technical Journal*, vol. 40, pp. 43–64, Jan. 1961.
- [22] D. Slepian, “Prolate spheroidal wave functions, fourier analysis and uncertainty–IV: Extensions to many dimensions; generalized prolate spheroidal functions,” *Bell System Technical Journal*, vol. 43, no. 6, pp. 3009–3057, Nov. 1964.
- [23] D. Slepian, “Prolate Spheroidal Wave Functions, Fourier Analysis, and Uncertainty –V: The Discrete Case,” *Bell System Technical Journal*, vol. 57, no. 5, pp. 1371–1430, Nov. 1978.
- [24] C. Zou, K. Kou, and Y. Wang, “Quaternion Collaborative and Sparse Representation With Application to Color Face Recognition,” *Preprint*.
- [25] P. Lucey, J. Cohn, T. Kanade, J. Saragih, Z. Ambadar, and I. Matthews, “The extended cohn-kanade database (CK+): A complete dataset for action unit and emotion-specified expression,” *2010 IEEE Computer Society Conference on Computer Vision and Pattern Recognition Workshops*, pp. 94–101, 2010.
- [26] T. Hupkens and J. Clippeleir, “Noise and intensity invariant moments,” *Pattern Recognition*, vol. 16, pp. 371–376, 1995.
- [27] J. Weston, S. Mukherjee, O. Chapelle, M. Pontil, T. Poggio, and V. Vapnik, “Feature selection for svms,” *NIPS.*, vol. 12, pp. 668–674, 2000.